Z. Phys. Chem. **225** (2011) 1343–1366 / **DOI** 10.1524/zpch.2011.0182

Diode Laser Induced Fluorescence for Gas-Phase Diagnostics

By Iain S. Burns[1,*] and Clemens F. Kaminski[2,3]

[1] Department of Chemical and Process Engineering, University of Strathclyde, Montrose Street, Glasgow, G1 1XJ, Scotland, UK
[2] Department of Chemical Engineering and Biotechnology, University of Cambridge, Pembroke Street, Cambridge, CB2 3RA, England, UK
[3] SAOT School of Advanced Optical Technologies, Friedrich Alexander University, 91058 Erlangen, Germany

Dedicated to Katharina Kohse-Höinghaus on the occasion of her 60th birthday

(Received September 8, 2011; accepted in revised form November 14, 2011)

Laser-Induced Fluorescence / Diode Laser / Spectroscopy / Gas-Phase Concentrations / Flame Temperature

We highlight the capabilities and potential of diode laser induced fluorescence for measurements in gas-phase reacting flows. Many applications of diode lasers in practical sensing are based on absorption spectroscopy. Fluorescence-based diagnostics possess similar advantages in terms of practicality and implementation-cost but additionally are capable of achieving excellent spatial resolution. Diode laser fluorescence instruments have been employed for high-sensitivity trace gas monitoring in applications ranging from plasma physics to atmospheric chemistry. This article begins by describing the UV-visible diode laser technology used to perform fluorescence. The principles of diode laser induced fluorescence are then reviewed and a comparison is made with absorption spectroscopy. Examples are given of concentration measurements of both atomic and molecular trace gases. Recent work on using diode laser induced atomic fluorescence for precision measurements of flame temperature is also reviewed. We conclude by a discussion of future opportunities for diode laser fluorescence spectroscopy drawing attention to interesting potential target species as well as novel application areas, such as monitoring of synthesis processes for nanomaterials.

1. Introduction

Diode lasers have become an important tool in the diagnostics of gas-phase systems both in research and in industry [1–4]. Measurements based on diode lasers have been applied to the study of combustion [4,5], atmospheric chemistry [6], plasma reactors [7], shock tubes [8] and chemical vapour deposition [7,9]. Applications have included measurements in industrial systems such as full-scale coal furnaces [10],

* Corresponding author. E-mail: iain.burns@strath.ac.uk

internal combustion engines [11] and detection of natural gas leaks [12]. Environmental monitoring using diode lasers has included the study of volcanoes [13], airborne measurements [14] and sensing of extra-terrestrial atmospheres [15]. Medical applications include breath analysis for diagnosis of asthma [16]. These examples illustrate the versatility of diode lasers that results from their low-cost and compact scale in addition to their wavelength-tuneability, stability and spectral purity. The robust nature of diode lasers makes them suitable for building field-deployable sensors and their narrow line-width enables highly sensitive and species-selective gas detection (including the measurement of isotope ratios [17]). Techniques exist for significantly enhancing the sensitivity of diode-laser absorption spectroscopy, including wavelength-modulation spectroscopy [18–20], cavity-enhanced absorption [21], cavity-ring down spectroscopy [22], balanced detection [23] and photo-acoustic spectroscopy [24].

The examples above involved absorption spectroscopy, which is the most common way of performing gas-phase diagnostics using diode lasers. In this article we concentrate instead on diode laser induced fluorescence. Fluorescence is a highly-sensitive technique for gas-phase measurements. Unlike absorption spectroscopy it is a spatially-precise measurement, allowing sharp gradients in reacting flows to be faithfully resolved. Laser-induced fluorescence has these unique advantages but because it depends on electronic excitation in the UV-visible spectral range, it has only been in recent years that its implementation with diode laser sources has become a realistic prospect. In the past, high-power pulsed sources such as Nd:YAG-pumped dye lasers have typically been used to excite narrow transitions of molecules in the gas phase for fluorescence detection. Diode laser absorption spectroscopy is usually performed in the near to mid infrared regions corresponding to ro-vibrational resonances in molecules and their overtones but these light sources are unsuitable for fluorescence experiments. The increasing availability of UV-visible diode lasers over the past decade has led to significant opportunities to use these compact light sources for fluorescence. It is therefore timely to review this new and expanding research field.

This article begins with an overview of the diode laser technology needed to work in the UV-visible wavelength region. Subsequent sections address the detection of atoms and molecules in low concentrations by diode LIF. The use of diode LIF as a temperature measurement technique is also covered and the levels of spatial-resolution and temporal-resolution that can be achieved are highlighted. Diode LIF has potential as a diagnostic technique for a wide range of gas-phase reacting flows and we give various examples here. We place an emphasis on measurements in flames since the steep gradients in temperature and concentration lead to a particular requirement for spatially-resolved diagnostics.

2. Diode laser technology

Instrumentation using diode lasers for absorption spectroscopy commonly exploits near-infrared technologies that were developed for the telecommunications industry [1]. The availability of single-mode tuneable diode lasers in this wavelength region led to their widespread use in gas concentration measurements: detection of H_2O, CO, CO_2, NH_3, CH_4, O_2, N_2O amongst many other small molecules has been reported [3]. Mod-

ifications to the standard diode laser were required to achieve the tuning properties necessary in these applications. Two notable designs of diode laser are the distributed feedback diode laser (DFB) and the vertical cavity surface emitting laser (VCSEL) [25]. The DFB laser incorporates a periodic modulation of refractive index into the diode laser, which leads to the selection of one particular longitudinal mode. The VCSEL, as the name implies, has mirrors above and below the active region, rather than at the ends. This results in a much shorter cavity with a correspondingly higher free spectral range, causing only one mode to be active within the diode laser gain profile. These lasers have favourable tuning properties but are restricted to certain spectral regions: while DFB lasers can be fabricated to emit at any wavelength between 760 nm and 2900 nm and at some wavelengths in the range 640–685 nm [26,27], VCSELs are only available in certain windows within the range 670–2050 nm [28,29].

The potential to employ these near-infrared diode lasers to perform fluorescence measurements was assessed by Li *et al.* [30], who studied an absorption transition in the $\nu_1 + \nu_3$ band of H_2O near 1392 nm. They report a very low fluorescence signal due to the low fluorescence quantum yield of the probed transition. The rate of spontaneous emission from the upper state (A) is only 89 s^{-1} [30] whereas the rate of quenching by N_2 (Q_{N_2}) is 1.4×10^4 s^{-1} $Torr^{-1}$ [30] and the rate of self quenching (Q_{H_2O}) is 7.5×10^5 s^{-1} $Torr^{-1}$ [30]. This allows the calculation of fluorescence quantum yield as a function of N_2 pressure:

$$\Phi = \frac{A}{A + Q_{N_2} + Q_{H_2O}} \tag{1}$$

Li *et al.* were able to detect weak fluorescence in a low-pressure cell by using a mechanical chopper and lock-in amplifier. Under these conditions (p_{H_2O}: 1 Torr; p_{N_2}: 0–35 Torr) a fluorescence quantum yield of between 1.2×10^{-4} and 7.2×10^{-5} would be expected. In practical measurement systems the fluorescence quantum yield would be much lower still. The authors estimate that for a typical composition of combustion products at atmospheric pressure, a laser power of about 70 W would be required for a practical tuneable diode laser fluorescence sensor. This power requirement substantially exceeds the typical output power of currently available diode lasers. The conclusion is not specific to this particular transition in water vapour but applies quite generally to the near infrared spectral region. Molecular transitions in the near infrared are usually weak overtone or combination bands.

As a consequence, the near ultraviolet and visible regions of the spectrum are much more attractive for diode laser induced fluorescence. These wavelengths correspond with strong electronic transitions of many atoms and molecules, resulting in much more favourable fluorescence quantum yields and therefore lower requirements on laser power. Nevertheless, single-mode tuneable diode laser sources are less readily available in the UV and visible. The inherently single-mode DFB and VCSEL devices described above do not currently exist for wavelengths below 640 nm. For this reason, alternative strategies must be adopted to obtain suitable sources for UV-visible fluorescence spectroscopy, including extended-cavity diode lasers and non-linear frequency conversion.

Opportunities for diode LIF arose due to the invention of blue diode lasers in the late 1990's [31]. These GaN sources provide access to a region of the spectrum that could previously only be reached with diode lasers by non-linear frequency conversion.

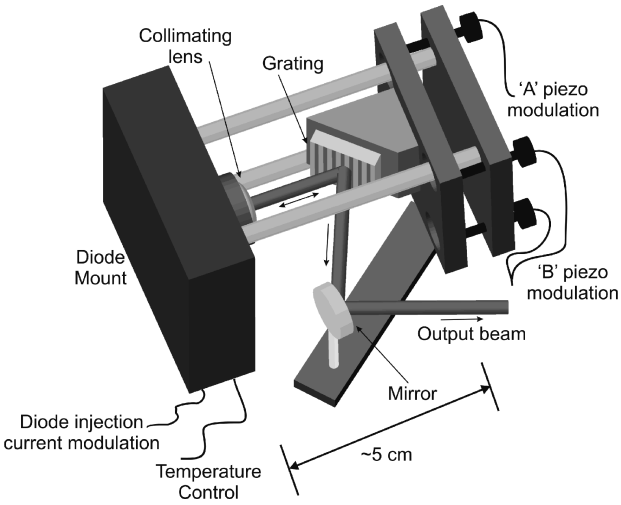

Fig. 1. An example layout for an extended-cavity diode laser.

Blue diode lasers are currently available in only some parts of the wavelength range 370–493 nm [32]. They are Fabry–Perot diode lasers, which emit multimode radiation because the gain bandwidth extends over several longitudinal modes. The spacing of these modes is defined as:

$$\delta\nu = \frac{c}{2nd\left(1+\left(\frac{\nu}{n}\right)\frac{dn}{d\nu}\right)} \tag{2}$$

where c is the speed of light, d is the cavity length, ν is frequency, n is the refractive index of the cavity. The dispersion term is often negligible but must be retained for certain diode laser materials. Fabry–Perot diode lasers can be coarsely wavelength tuned by adjusting the temperature or driving current, but the multimode emission is not suitable for high-resolution spectroscopy. Extended-cavity diode lasers (ECDL) are built by using a grating (or sometimes another component) to retro-reflect a part of the output beam back into the diode cavity [33–35], as shown in Fig. 1. This gives rise to a second set of modes resulting from the cavity formed by the grating and the back facet of the diode.

The extended cavity and diode modes of an ECDL are shown schematically in Fig. 2, together with the grating feedback profile and the diode gain profile. When correctly aligned, the retroreflection from the grating favours one of the diode modes. These laser sources have found application in many practical diagnostic applications since they are a relatively convenient way of obtaining wavelength-tuneable, single-mode radiation in the visible region of the spectrum.

Wavelength tuning of extended-cavity diode lasers involves tuning of the extended-cavity modes, as well as the grating feedback profile. This is done by simultaneously translating and rotating the grating. To maintain an overlap between the grating feedback profile and the active extended cavity mode it is necessary to translate and rotate the grating in the correct proportion. This has often been done by using a single piezo-

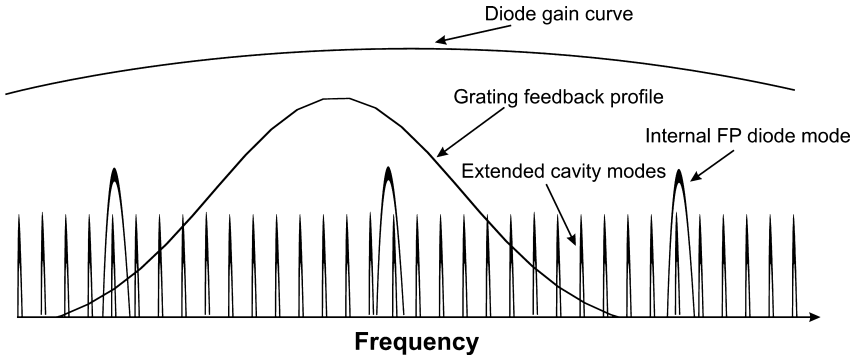

Fig. 2. Schematic representation of mode competition in an ECDL.

electric actuator to rotate the grating around a pivot point whose location is optimised to fulfil the constraint [36]. This involves a delicate mechanical optimisation and also does not permit the initial overlap of the extended cavity mode and grating feedback profile to be finely adjusted. A more favourable approach involves the use of a multi-piezo mount, which allows the magnitudes of rotation and translation of the grating to be controlled independently [37,38].

Many extended cavity diode laser designs have involved application of anti-reflection coating to the front facet of the diode laser to suppress the diode modes [39]. This adds to the complexity and cost of the laser system and it is beyond the capabilities of most applied laser diagnostics laboratories to perform this in-house. Furthermore, previous work established that the internal modes of blue-violet diode lasers could not be adequately suppressed by application of anti-reflection coating and that synchronous tuning of the diode laser injection current (to adjust the cavity length by resistive heating) was necessary to achieve a favourable mode-hop free tuning range [40]. Various other researchers have combined pivot-point grating tuning and diode current tuning [35,41]. The present authors combined current tuning with multi-piezo tuning using a standard reflection grating to construct ECDLs entirely from commercially available components [42,43]. Blue-violet ECDLs at wavelengths near 410 nm and 451 nm both achieved mode-hop-free tuning ranges in excess of 90 GHz [42,43] (*i.e.* 3 cm^{-1} or > 50 pm), exceeding the performance of previous blue-violet ECDLs and commercially-available systems.

Some applications require locking of the wavelength of the ECDL to coincide with the peak of the absorption line being probed. This is a way of optimising signal-to-noise ratio in cases when signal levels are weak. It is also required when the objective is to monitor dynamics faster than the maximum wavelength tuning rate of the ECDL. Various strategies have been demonstrated for wavelength-locking to the peak or flank of a reference absorption line [44] or locking by feedback from high-finesse cavity [45]. In the case where an optical cavity is used, drifts in its temperature and pressure must be avoided to achieve good wavelength stability. In the fields of precision metrology and ultra-high-resolution spectroscopy, where ECDLs based on the same principles are employed, there are exacting demands on laser stability: advanced techniques have been developed to achieve locking to within a fraction of 1 Hz [46,47].

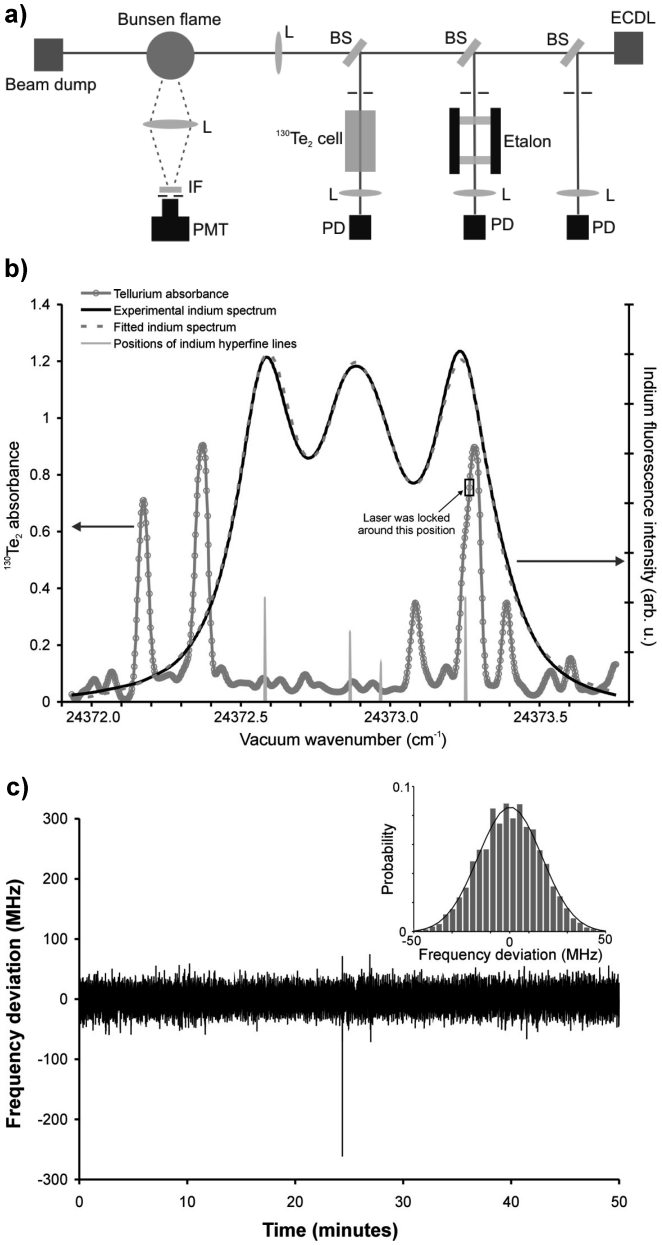

Fig. 3. a) Experimental set-up for wavelength-locking of a 410.18 nm ECDL to a tellurium vapour reference line and using the locked laser to perform fluorescence of indium in a flame; **b)** spectra of tellurium and indium showing the position at which the laser was locked to a tellurium line; **c)** variation in frequency of the actively locked diode laser: the variation was calculated from the fluctuations in the intensity of the laser beam transmitted through the $^{130}Te_2$ absorption cell. Insert: histogram of deviations from the mean laser frequency with a Gaussian fit. (PMT: photomultiplier tube; IF: interference filter; L: lens; BS: beam splitter; PD: photodiode; ECDL: extended-cavity diode laser) [49].

For gas-phase sensing, where the requirements are not so stringent, simpler schemes suffice. A tellurium containing vapour is suitable reference gas in blue/near UV spectral region since it has a dense spectrum of strong absorption lines [48]. Active wavelength-locking of an ECDL has been performed by monitoring the transmission through a glass cell containing tellurium heated to about 600 °C in a ceramic furnace [49], as shown in Fig. 3a. The laser was tuned to the flank of a strong absorption line so that slight drifts in wavelength resulted in changes in the transmission intensity (see Fig. 3b). Feedback control was implemented by adjusting the piezo voltage offset to bring the transmitted intensity back to the set-point [49]. A plot of the frequency deviation of the locked laser as a function of time is shown in Fig. 3c, together with a histogram specifying the wavelength stability. It can be seen from Fig. 3 that the laser remained locked for 50 min with a stability of about ±25 MHz. These variations in frequency of the locked laser correspond to a variation in tellurium absorbance of only ±1.5% of the peak value (the full-width at half-maximum height of the tellurium line identified in Fig. 3b is about 1.8 GHz). This is certainly adequate for practical gas-phase diagnostics since transition linewidths at atmospheric pressure and room temperature are typically at least several GHz. The use of a hollow cathode lamp containing a suitable metal such as indium is a way to achieve ECDL wavelength locking while avoiding the need for a high-temperature furnace [50], although at the expense of a much narrower available wavelength range for locking.

The wavelength-tuning rate of external cavity diode lasers is ordinarily limited to about 100 scans per second due to the requirement for mechanical movement of the grating. The rate of tuning that can be achieved is dependent on the mass being displaced by the piezo actuators. This limitation has been overcome by placing a wedge-shaped electro-optic modulator within the laser cavity to deflect the beam [51], but this substantially increases the complexity and cost of the device. Kranendonk *et al.* demonstrated a wavelength tuning rate of 15.5 kHz in the near infrared by constructing a modeless ECDL [52]. The extended cavity modes were suppressed by placing a resonant scanning mirror within the cavity: this resulted in a linewidth as large as 0.3 nm, useful for measurements at elevated pressure but not capable of fine spectral resolution.

We have developed another approach for high-speed wavelength tuning of ECDLs that does not require the use of additional optical components and avoids the need for mechanical movement of the grating [53]. Instead of attempting to match the modes of the external cavity with the diode modes, the grating is left stationary and only the laser current is tuned. Therefore, only the diode modes shift in frequency during tuning (see Fig. 2). If the transition being probed is narrower than the spacing between diode modes then only one diode mode is on resonance with the analyte. As the diode current is tuned, one of the other diode laser modes will soon overlap better with an extended-cavity mode. At this point, a mode-hop occurs. The emission wavelength jumps from the on-resonance mode to other modes and back again as the laser is tuned. This results in a fluorescence or absorption spectrum like the one shown in Fig. 4. The regions where the on-resonance mode is active result in a fluorescence signal. In the intervening regions, where the active mode is off-resonance, no signal is detected. The spacing between the positions where the on-resonance diode mode is active is equal to the free spectral range (FSR) of the extended cavity. These on-resonance regions give data-points that can be fitted to a theoretical spectrum. It can be advantageous to work

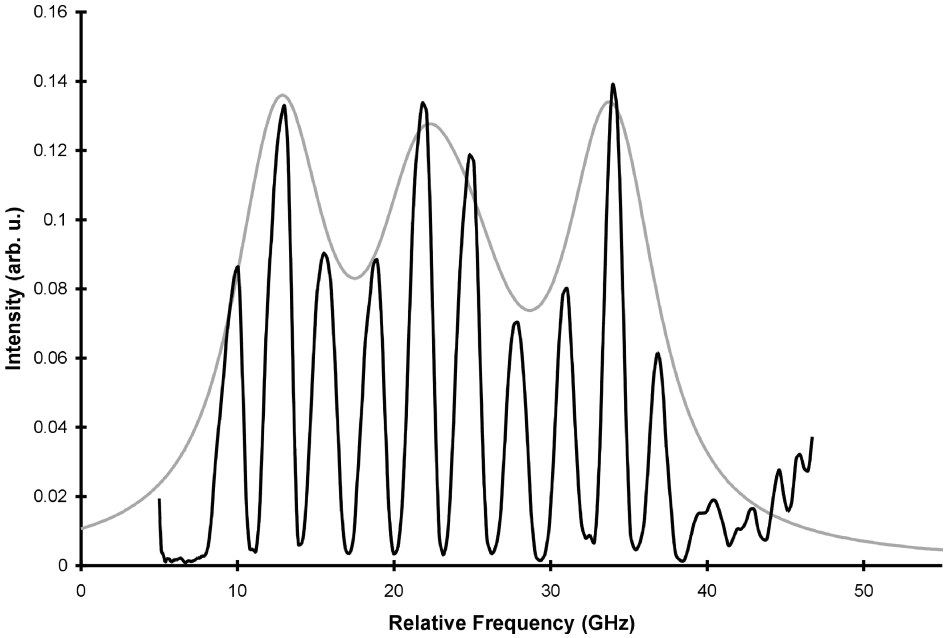

Fig. 4. The dark trace shows the fluorescence recorded for a single scan over the $5^2P_{1/2} \rightarrow 6^2S_{1/2}$ transition (410.18 nm) of atomic indium in a flame performed in a time of 100 μs by tuning only the injection current of the ECDL. The spectrum is modulated since the ECDL switches between the on-resonance mode and other modes during tuning. The peak positions on this trace were extracted to form the fluorescence spectrum and a theoretical spectrum (shown in light grey) was fitted to this data. The concentration of indium in the flame was estimated to be in the region of 10 ppb [53].

with a somewhat longer extended cavity (*i.e.* lower FSR) to improve the spectral resolution. Tuning rates exceeding 10 kHz were thus achieved. Although we demonstrated this rapid ECDL tuning for an isolated atomic transition whose linewidth is narrower than the diode mode spacing, further development could make it suitable to the study of more complex spectra.

This method shares some conceptual similarity with the multi-mode absorption spectroscopy (MUMAS) approach, developed by the Ewart group [54,55], where a Fabry–Perot diode laser is used without an extended cavity. The MUMAS spectrum is a sum of contributions of several laser modes. Fitting to a theoretical spectrum calculated from the mode spectrum of the laser and the simulated absorption spectrum is necessary to determine gas concentrations from the data [54].

Some applications require wavelengths where no diode lasers are currently available, such as below 370 nm or in some parts of the region between 370 to 493 nm where conventional GaN diode laser technology exhibits wavelength gaps. Tuneable laser radiation at wavelengths where no diode laser is available can be generated by second harmonic generation (SHG) or sum-frequency mixing (SFM) using non-linear crystals. Before blue diode lasers were available, SHG was used to generate radiation at 426 nm for detection of CH in flames [56]. Sum-frequency generation can be done with

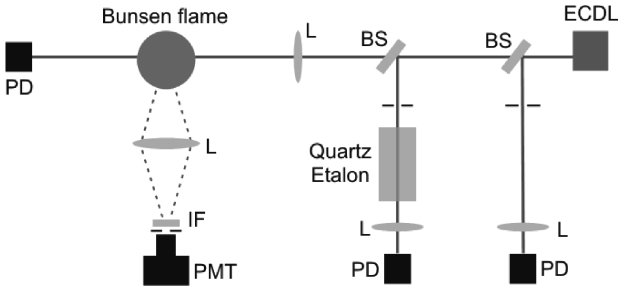

Fig. 5. Experimental set-up for the simultaneous acquisition of fluorescence and absorption spectra of atomic indium. (L: lens; IF: interference filter centred around 451 nm; PMT: photomultiplier tube; PD: photodiode; BS: beam splitter; ECDL: extended-cavity diode laser).

two diode lasers, or by mixing a diode laser with a diode-pumped solid state laser or argon-ion laser. Non-linear frequency conversion of diode laser radiation has also been employed in numerous gas-sensing studies including some examples of fluorescence spectroscopy, in order to probe strong electronic transitions in the UV. A further discussion of such light sources is part of Sect. 5.2 below, which deals with the detection of molecular species by diode laser induced fluorescence.

3. Principles of diode laser induced fluorescence

The general principles of laser-induced fluorescence applied to gas-phase diagnostics have been covered extensively elsewhere [57–61]. The objective here is to draw attention to features that are particular to diode laser induced fluorescence. The diode laser sources described above have narrow linewidths of less than 10 MHz, meaning that atomic and molecular spectra can be well-resolved (transition linewidths are typically a few GHz at ambient pressure). By contrast, this is usually not possible with standard pulsed dye lasers, whose linewidth is generally in the range 1–10 GHz. Another advantage of diode lasers is their relatively rapid wavelength tuning compared to typical dye lasers, which are tuned mechanically by displacing a large grazing-incidence grating.

The set-up of a diode laser fluorescence experiment is shown in Fig. 5. The diode laser beam is directed through a gas sample and some of the light is absorbed if it coincides with the wavelength of a resonance of atoms or molecules in the sample. This results in the emission of fluorescence, which is usually collected on an axis perpendicular to the beam propagation direction. The collection lens images the fluorescence signal onto the detector. Photomultiplier tubes are generally used for detection of diode laser induced fluorescence in the visible spectral region due to the relatively low signal levels, but CCD cameras have also been used [62]. The spatial resolution of the measurement is defined by a cylinder with diameter of the beam waist at the focus and length determined by the width of the pin-hole or other aperture placed in the focal plane of the collection lens. An etalon can be used to verify that the tuning is mode-hop free and to calibrate the wavelength scale of the scan. Filters or a monochromator are used to discriminate against background light such as flame emission.

The optical power of the collected fluorescence signal, S_F (photons s^{-1}), is:

$$S_F = \frac{I(\nu)}{h\nu} A_L (1 - e^{-N_1 \sigma_{12} l}) \cdot \Phi \cdot \frac{\Omega}{4\pi} \eta \tag{3}$$

where $I(\nu)$ is the incident laser irradiance (W cm^{-2}), A_L is the cross-sectional area of the interrogation region, N_1 (cm^{-3}) is the population of molecules in the lower state of the probed transition, $\sigma_{12}(\nu)$ is the absorption cross-section of the probed transition at the laser frequency, l is the length of the interrogation region, Φ is the fluorescence quantum yield, Ω is the collection solid angle and η is the detection efficiency accounting for the fractional transmission of the signal collection optics and filters and the quantum efficiency of the detector. Since the fractional absorption over the interrogation region is usually low, we can use the approximation, $1 - e^{-x} \approx x$ to obtain:

$$S_F = \frac{I(\nu)}{h\nu} V_L N_1 \sigma_{12}(\nu) \cdot \Phi \cdot \frac{\Omega}{4\pi} \eta \tag{4}$$

where V_L is the volume of the interrogation region. This equation can be grouped into factors representing the rate of absorption, the fluorescence quantum yield and the fraction of the signal detected. In this way, the fluorescence signal is proportional to the fractional absorption within the measurement volume. It is also proportional to the number density of the analyte, although this linear relationship breaks down in the case of strong absorption of the incident beam or signal trapping. Saturation of the probed transition (*i.e.* significant depopulation of the ground state) occurs at high laser irradiance but is unlikely to be achieved using continuous wave diode laser excitation sources other than at very low pressure.

The rate of absorption is dependent on the incident wavelength and on the lineshape of the probed transition. The transition lineshape is a function of temperature and pressure due to the effects of temperature (Doppler broadening) and pressure (collisional broadening) [57,59]. The fluorescence quantum yield is highly dependent on the rate of quenching or other non-radiative losses from the excited state. The rate of collisional quenching is a roughly linear function of pressure and is strongly influenced by temperature and composition.

4. Comparison to absorption spectroscopy

Fluorescence is almost always much more sensitive than simple single-pass absorption spectroscopy. The fluorescence signal strength is much weaker than the intensity of the transmitted beam, but the sensitivity of the fluorescence technique results from the fact that it is a zero-baseline method. Absorption spectroscopy, by contrast, involves measuring small fractional deviations in a strong signal. Laser noise therefore has much more influence on absorption spectroscopy than on fluorescence: a ripple of $\pm 0.1\%$ in the laser power would significantly compromise the direct measurement of 0.01% absorption but would be of little consequence to a fluorescence measurement. Various approaches are available to enhance the sensitivity of absorption spectroscopy either by increasing the fractional absorption and/or by noise cancellation and these have been referred to above. The detection limit of such techniques is often quoted in

$cm^{-1}\,Hz^{-1/2}$ [63]. This is based on the assumption that the measurement is limited by white noise so that the detection limit will scale with the square root of signal integration time. This assumption can be tested by plotting the Allan variance of the signal as a function of integration time [64]. The detection limit also scales linearly with the optical path length.

It is difficult to compare the sensitivities of fluorescence and absorption techniques in a meaningful fashion as they depend on the practical details of a specific experiment. The most favourable conditions for fluorescence are low temperature and low pressure, resulting in narrow spectral lines and a high quantum yield. The detection sensitivity can be increased by using large measurement volumes, which comes at the expense of spatial resolution. The f-number of the signal collection optics is crucial in LIF. For example, use of a 50-mm-diameter lens situated 120 mm from the measurement volume would result in collection of only about 1% of the emitted photons from the imaged region. In the case of low signal-levels, a concave mirror can be used to refocus fluorescence at the measurement volume which results in roughly double the collection efficiency [30].

It should be noted that fluorescence does not provide an inherently absolute measure of concentration. According to Eq. (4) above, the fluorescence signal is linearly proportional to the number density of the analyte. As previously discussed, however, it is also dependent on the rate of quenching from the upper state, which is a function of temperature, pressure and composition. To make the measurement absolute, either knowledge of quenching cross-sections at the relevant conditions (which can be determined, for example, by fluorescence lifetime measurements) or an external calibration is required (see *e.g.* [65]). In some cases calibration may be achievable by comparing direct absorption and fluorescence measurements from a reference gas at high concentration before taking advantage of the favourable detection limit of fluorescence in a trace gas measurement. Accurate calibration is often not needed as in many applications one is mainly interested in relative concentration changes in time, compared to some reference condition.

Another advantage of fluorescence is that it is a spatially resolved technique. This provides the potential for practical monitoring of dynamic systems such as flames and exhausts and to investigate the fine structure (a resolution of less than $\sim 100\,\mu m$ is readily achievable) of flames at high repetition rates. Absorption spectroscopy can be combined with tomographic reconstruction to give a certain level of spatial resolution [66] and this has proved useful in some applications, but the spatial fidelity is a long way from what can be achieved with fluorescence.

Although a direct comparison between fluorescence and absorption is not straightforward, it would appear that UV-visible diode laser fluorescence is at least as sensitive as wavelength-modulation absorption spectroscopy under harsh flame conditions and has the potential to be considerably more sensitive at low temperature and pressure and with a larger measurement volume. Under such conditions, it could be competitive with cavity-based absorption techniques but at substantially improved temporal and spatial resolution. Diode laser fluorescence has the advantage over such approaches that it does not require costly high-reflectivity mirrors and it does not suffer the experimental complexity associated with the alignment of optical cavities. The need to use grating-feedback to perform high-resolution diode laser spectroscopy in the UV-visible spectral

region of course applies to cavity-based absorption methods as well as to fluorescence measurements.

In the subsequent sections we provide examples to illustrate the range of applications for UV-visible diode laser enabled fluorescence measurements and point towards potential future developments.

5. Applications

Diode laser excited fluorescence has been used for the detection of atoms and small molecules in a range of gas-phase systems, including flames, plasmas and the atmosphere. In this section we summarise this work and draw attention to opportunities for extending to new target species and measurement systems, including measuring precursor concentrations in nanomaterials synthesis processes.

5.1 Atomic fluorescence

Gas phase atomic species are prime candidates for detection by gas-phase atomic fluorescence measurements because many of them have electronic transitions in the UV-visible region with oscillator strengths typically two or three orders of magnitude greater than those of small molecules. This leads to high fluorescence quantum yields according to Eq. (1), even at elevated temperature and atmospheric pressure. A previous review by Galbács [67] covered the application of diode lasers to atomic spectroscopy, although it was mainly concerned with absorption measurements. Several examples of diode laser atomic fluorescence have involved sensing of metal atoms. Some of these are summarised in Table 1, which highlights information about previous practical sensing using diode lasers.

Atomic spectroscopy in flames provides vital data in the study of combustion, in particular through measurement of flame temperature [79]. Flames are also used for the atomisation of solutions to determine concentrations of dissolved metals [76]. In other cases, a laboratory flame is used to generate hot exhaust gases for the purpose of developing and validating techniques for monitoring of heavy metal pollutants [73].

Combustion is a significant research field since it continues to be the dominant source of energy. The formation of pollutants such as soot and NO_x in flames is not well understood at present and progress in this area would allow better prediction, and thus minimisation, of harmful emissions from engines and furnaces [80]. Temperature is a critical parameter in the understanding of combustion due to its non-linear influence on reaction rates. It is difficult to measure with the required accuracy, in particular in rich flames where soot is formed. Good spatial resolution is required due to the steep spatial gradients present in flames: this makes fluorescence a suitable choice. Various other optical techniques for flame temperature measurement exist but many of these are ill-suited to low-pressure or sooting flames or limited to low repetition rates as we have discussed elsewhere [50,79,81].

Flame temperature measurements based on two-line atomic fluorescence (TLAF) were first performed using flash-lamps or dye lasers as excitation sources [82,83]. Dye lasers were then used to perform temperature imaging in flames and in en-

Table 1. Applications of diode lasers to atomic fluorescence and absorption spectroscopy in the UV-visible spectral region.

Species	Transition	Wavelength	Absorption	Fluorescence
Mercury	$6^1S_0 \rightarrow 6^3P_1$	253.7 nm	Vapour cell [68] Vapour cell [69] Vapour cell; coal-fired combustor exhaust [70]	
Aluminium	$3^2P_{1/2} \rightarrow 4^2S_{1/2}$	394.4 nm	Physical vapour deposition process [71]	
Gallium	$4^2P_{1/2} \rightarrow 5^2S_{1/2}$ $4^2P_{3/2} \rightarrow 5^2S_{1/2}$	403.30 nm 417.20 nm	Hollow-cathode lamp [72]	Atomic beam [72]
Indium	$5^2P_{1/2} \rightarrow 6^2S_{1/2}$ $5^2P_{3/2} \rightarrow 6^2S_{1/2}$ $5^2P_{3/2} \rightarrow 5^2D_{3/2}$ $5^2P_{3/2} \rightarrow 5^2D_{5/2}$	410.18 nm 451.13 nm 325.61 nm 325.86 nm	 Flame [73] Flame [73]	Flame [74] Flame [42]
Copper	$4^2S_{1/2} \rightarrow 4^2P_{3/2}$	324.75 nm	HCL; dc plasma; flame [73]	
Cadmium	$5^1S_0 \rightarrow 5^3P_1$	326.11 nm	Flame [73]	
Rubidium	$5^2S_{1/2} \rightarrow 5^2P_{3/2}$	780.0 nm	Industrial furnace [75]	Flame [76]]
Potassium	$4^2S_{1/2} \rightarrow 5^2P_{3/2}$ $4^2S_{1/2} \rightarrow 5^2P_{1/2}$ $4S_{1/2} \rightarrow 4P_{3/2}$ $4S_{1/2} \rightarrow 4P_{3/2}$	404.5 nm 404.78 nm 766.49 nm 769.90 nm	Vapour cell [77] Vapour cell [77] Industrial furnace [75] Industrial furnace [75]	Vapour cell [77] Vapour cell [77]
Lithium	$2^2S_{1/2} \rightarrow 2^2P_{3/2}$	670.78 nm		Inductively-coupled plasma [78]
Ytterbium	$6^1S_0 \rightarrow 6^1P_1$	398.9 nm	Hollow-cathode lamp [44]	

gines [84–86]. Diode laser excited atomic fluorescence has subsequently been developed [87] with the two key objectives: (i) to make temperature measurements in sooting flames with sufficient accuracy and precision to contribute to understanding of flame chemistry [79]; (ii) to make kHz-repetition-rate measurements in flames to resolve rapid dynamics [50].

The method is based on probing the relative population of the two spin-orbit-split sublevels of the ground state of atomic indium seeded to flames. Indium is selected as the probe species because the separation between these levels is 2213 cm^{-1} [88], which is roughly equal to kT at flame conditions and thus leads to near-optimal temperature sensitivity. Extended-cavity diode lasers emitting near 410.18 nm and 451.13 nm are used sequentially to probe the $5^2P_{1/2} \rightarrow 6^2S_{1/2}$ and $5^2P_{3/2} \rightarrow 6^2S_{1/2}$ transitions of indium respectively. Our work has involved the use of a single detector fitted with a band-pass filtered transmitting at 451 nm [87]; this means that resonance fluorescence is collected for the $5^2P_{3/2} \rightarrow 6^2S_{1/2}$ excitation. Nevertheless, no interference from elastic scattering has been observed, even in sooting flames [79].

Most of the diode-laser TLAF measurements have been performed by wavelength-scanning the two blue diode lasers to record fluorescence spectra of the two indium transitions [79,87]. The diode laser beams are overlapped and focussed at the flame central axis. The fluorescence generated in the focal region is imaged on a perpendicular axis through an interference filter and pin-hole onto a photomultiplier tube. The fluorescence spectra are normalised by the simultaneously-recorded laser power and fitted with a theoretical spectrum representing the hyperfine components of the respective transitions [87]. The integrals of the fitted spectra are used to determine temperature, T, based on the following equation [79]:

$$T = \frac{\Delta E/k}{\ln\left(\dfrac{\int_0^\infty \dfrac{F_a(\nu)}{I_{13}(\nu)}d\nu}{\int_0^\infty \dfrac{F_b(\nu)}{I_{23}(\nu)}d\nu}\right) + 3\ln\left(\dfrac{\lambda_{32}}{\lambda_{31}}\right) + \ln\left(\dfrac{A_{32}}{A_{31}}\right)} \tag{5}$$

where ΔE is the energy spacing between the ground states of the probed transitions, F_a and F_b are the fluorescence intensities resulting from 410 nm and 451 nm excitation respectively, I_{13} and I_{23} are the excitation intensities, λ_{31} and λ_{32} are the transition wavelengths, A_{31} and A_{32} are the rates of spontaneous emission and k is the Boltzmann constant.

The first demonstration of diode laser TLAF established the principle of the technique [87] but careful work was required to achieve the accuracy and precision required to contribute to detailed studies of soot formation in laminar flames [79]. Atomic indium is seeded to the flame *via* a spray-type nebuliser containing an aqueous solution of indium chloride. Early diode laser TLAF experiments were affected by drifts in the seeded indium concentration, which caused a bias in the signal ratio thus leading to errors in the measured temperature. Efforts to stabilise the concentration of seeded indium did not minimise this error source sufficiently. Instead, the technique was modified by interleaving the wavelength scans of the two diode lasers through use of a mechanical chopper [79]. This allowed fifty single-scan spectra to be recorded for each laser in a time of five seconds. Any drifts in indium concentration in the flame are expected to be random and uncorrelated to the switching between the two laser beams. The temperature determination was done by averaging the fifty spectra recorded for each laser. This procedure therefore makes the measurement immune to drifts in indium concentration.

Other experimental errors can stem from imperfect overlap between the two diode laser beams and inaccurate measurement of the excitation intensities. In our most recent work the careful minimisation of these error sources led to an accuracy of ±41 K and precision of ±8 K in the soot formation region of a low-pressure laminar flame at temperatures in the region of 1700 K [79]. These levels of accuracy stem from the highly resolved fluorescence spectra that can be recorded with blue diode lasers. Atomic indium is seeded to the flame in trace quantities (∼ 10 ppb). Any influence of the seeding process on flame temperature is therefore minimal. An upper estimate of this error source was made previously [81] by performing thermocouple measurements in the

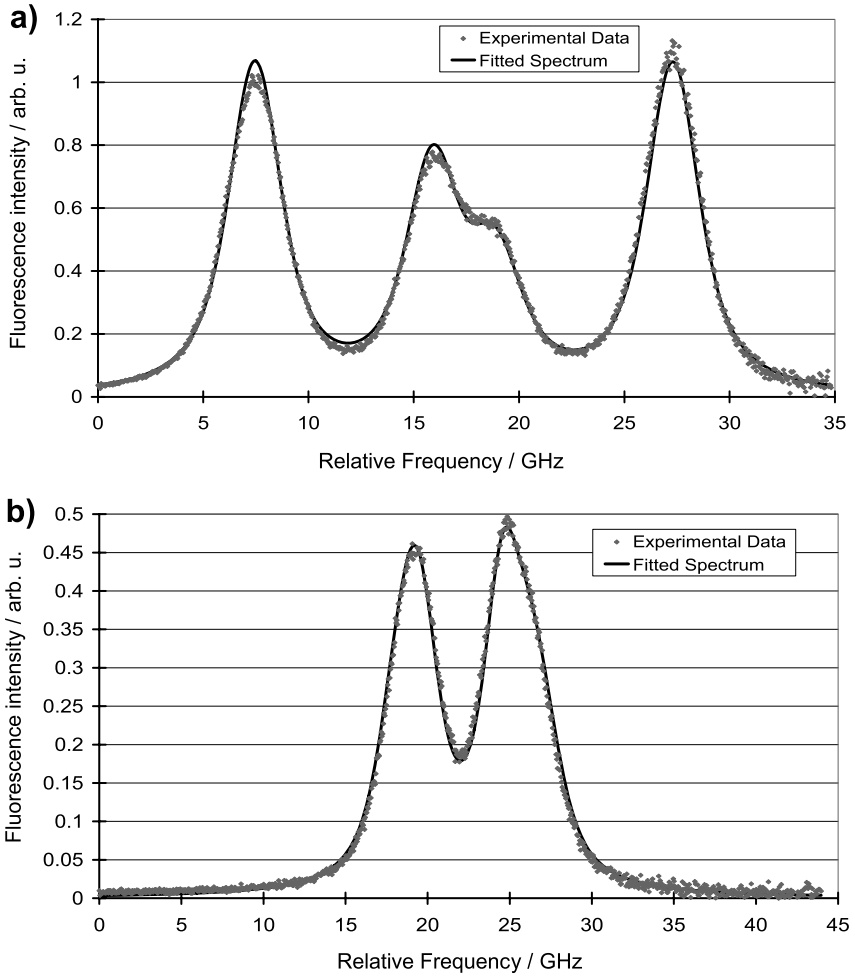

Fig. 6. Fluorescence spectra of atomic indium with excitation by tuneable diode lasers at 410.18 nm **a)** and 451.13 nm **b)**. The spectra were recorded in a low-pressure (26.7 kPa) sooting flame with fuel equivalence ratio of 2.32 (mole fractions: CH_4: 0.46; O_2: 0.40; N_2: 0.14) at 40 mm above the burner surface at a temperature of 1590 K. These are averaged spectra resulting from fifty interleaved wavelength scans [79].

presence and absence of seeding and this contributes to the estimated uncertainty of ±41 K [79].

Examples of the averaged fluorescence spectra recorded in a low-pressure sooting flame are shown in Fig. 6, where excellent agreement to theoretical fits is apparent. The different appearance of the 410.18 nm spectrum from the ones shown in Figs. 3 and 4 is a consequence of the reduced pressure. The resulting temperatures are shown in Fig. 7, which presents measurements taken in low-pressure sooting flames of two different equivalence ratios. The spatial resolution in the vertical direction was 100 μm. The precision of the results is sufficient to reveal subtle differences between the tempera-

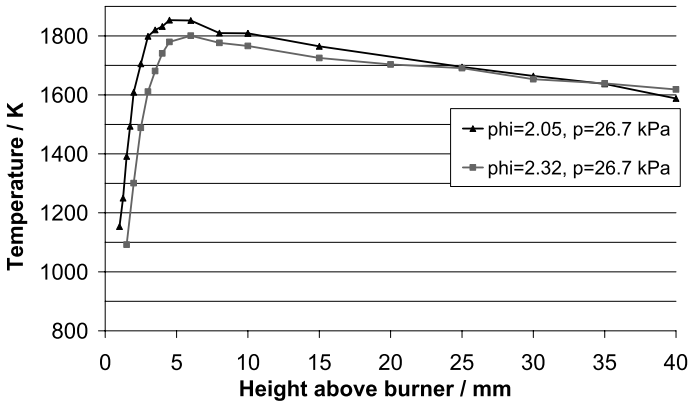

Fig. 7. TLAF temperature measurements in laminar premixed sooting flames at a pressure of 26.7 kPa stabilised on a 60 mm-diameter McKenna burner. The flames had fuel equivalence ratios of 2.05 (mole fractions: CH_4: 0.434; O_2: 0.425; N_2: 0.14) and 2.32 (mole fractions: CH_4: 0.46; O_2: 0.40; N_2: 0.14). For both flames the total flowrate of premixed reactants was 4.11 standard litres per minute (slpm). The favourable precision (±8 K) is evident from the temperature profiles and allows slight differences between the two flames to be distinguished [79].

ture profiles of the two flames, the less rich one situated closer to the burner surface and having a slightly higher maximum temperature. These measurements provide important data for the understanding of soot formation that could not have been obtained by other means. The results have also been vital for the interpretation of other experimental data recorded in the same flames [89,90]. It should be noted that temperature measurements could not be obtained below about 1000 K due to the low vapour pressure of indium chloride under those conditions.

In addition to optimisation of precision and accuracy for the investigation of pollutant formation in laminar flames, another major goal was to develop a high-speed diode laser TLAF system for the study of rapid flame dynamics. A different experimental approach was required to achieve the temporal resolution desired. The high-speed wavelength scanning of ECDLs described in Sect. 2 [53] yields an improvement but even faster temperature measurements can be performed using ratiometric measurements at fixed laser wavelengths locked to the peaks of the indium transitions. This also allows signal levels to be maximised and therefore leads to optimal precision. Wavelength stability is crucial here and was achieved by locking the laser wavelengths to the flanks of absorption lines in an In-containing hollow-cathode lamp as described in Sect. 2. A mechanical chopper was used to switch between the excitation beams at kHz repetition rates [50,91]. An example of the raw data recorded by this technique is shown in Fig. 8.

The calculation of temperature from the signal levels is not as simple as in the case of wavelength scanning TLAF. Here we record not line-integrated fluorescence but the fluorescence generated at fixed wavelengths near to the peaks of the indium transitions meaning that Eq. (5) cannot be used directly for the calculation of temperature. Instead it is necessary to model the indium transition line-shapes and line-shifts as a function of temperature (and pressure). Since the wavelengths of the locked lasers are known, this

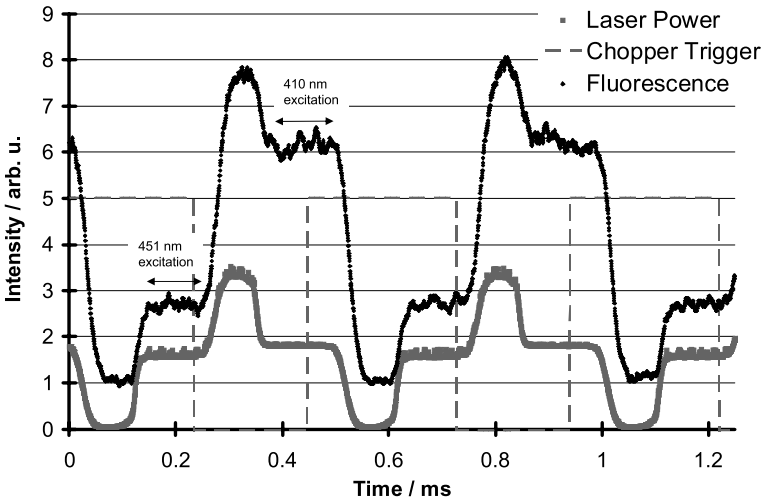

Fig. 8. Example of raw data for high-repetition rate TLAF. The ratio of normalized fluorescence signals is used to calculate flame temperature. In this case, two temperature measurements were recorded per millisecond [91].

allows the measured ratio of fluorescence signals to be used to determine flame temperature [50,91]. Temperature measurements have been demonstrated with a precision of 1.5% and spatial resolution of 150 μm at a repetition rate of 3.5 kHz in acoustically pulsed laminar flames [50], thus illustrating the potential for TLAF to be used for the study of dynamic flame behaviour.

As well as ratiometric temperature measurements, it is also possible to use fluorescence lineshapes to determine temperature. This leads to the possibility of making spatially resolved measurements of flame temperature using a single diode laser. This avoids the need for careful overlap of two diode laser beams discussed above and results in a simpler experimental setup. Fluorescence lineshape temperature measurements have been demonstrated both in atmospheric-pressure [92] and low-pressure flames [81]. An uncertainty of ±45 K was estimated for the measurements in low-pressure flames at 5.3 kPa. The accuracy is slightly less good at atmospheric pressure due to the more significant contribution of collisional broadening, whose dependence on temperature is less straightforward than that of Doppler broadening. Considerably larger experimental errors are expected at intermediate pressures of around 20–30 kPa, where the contributions of Doppler and collisional broadening are comparable and the overall transition lineshape shows little sensitivity to temperature. We therefore recommend that evaluation of temperature based on fluorescence lineshape offers a convenient alternative to TLAF, which can work quite well under certain conditions. The two-line thermometry approach is nevertheless the way to achieve the best possible precision and accuracy over a wide range of flame conditions.

We have focussed here on the use of atomic fluorescence to measure flame temperature but similar temperature measurements could be performed in other high-temperature reacting systems. Concentration measurements by atomic fluorescence are

of relevance to a range of technical applications with a notable example being nanomaterials synthesis processes. The examples in Table 1 include atomic spectroscopy in flames, vapour deposition processes, atomic beams and plasmas. All of these systems are of interest in the synthesis of advanced functional nanomaterials, which often consist of metal or metal oxide nanoparticulates or thin films, and have widespread uses such as in catalysis, energy storage, photovoltaics and biomedical applications [80]. There has been recent work on imaging of iron atom concentrations in a low-pressure flame used for the synthesis of iron oxide nanoparticulates using a Raman-shifted excimer laser [93]. The use of diode lasers for atom concentration measurements in such nanomaterials synthesis processes offers the potential for much more compact and cost-effective diagnostics. There is a pressing requirement for such experimental data since the mechanisms involved in nanoparticle formation in flames and in plasmas is not currently well-understood. Better predictive capabilities are needed to tailor the properties of functional nanomaterials for specific applications and for scaling up production. Sensors based on diode laser fluorescence also have the potential to be used for on-line monitoring and control of nanomaterials synthesis.

5.2 Molecular fluorescence

We have already noted that molecules have much lower oscillator strengths than atoms, leading to weaker fluorescence signals. Nevertheless, diode laser induced fluorescence has been demonstrated for a few practical applications, including in high-temperature reacting flows. This seems to indicate potential for further uses of diode LIF for detection of molecular species in trace quantities. A summary of applications of diode LIF to concentration measurements of various molecules is given in Table 2. There have been notable applications of diode LIF in combustion diagnostics and atmospheric chemistry research. The table also includes details of some measurements by sensitive UV-visible diode laser absorption spectroscopy as an indication of future opportunities for fluorescence measurements.

It is interesting to note that laser induced fluorescence of CH radicals in a flame was already demonstrated in 1999 [56], prior to the widespread availability of blue diode lasers. Blue light at 426 nm was generated by frequency doubling a near infrared diode laser. The resulting output power was only 100 μW but this was sufficient to perform CH LIF in a Wolfard-Parker slot burner by wavelength modulation spectroscopy [56]. This early proof-of-principle for diode LIF in flames has not been followed by subsequent studies of radical concentrations in flames and the current availability of blue diode lasers opens the potential to build compact instruments at a fraction of the cost of traditional dye laser systems. The same group also demonstrated diode laser fluorescence detection of OH radicals in a low-pressure discharge flow reactor by sum-frequency mixing of a near infrared diode laser with an argon-ion laser [100] to generate about 1.5 μW of UV radiation at 308 nm. The availability of higher output powers in the UV by more efficient frequency doubling and mixing of diode laser sources may make it possible to extend the detection of radicals in flames by diode LIF to OH, which is important as a marker of flame-front location and can also be used for flame thermometry.

Table 2. Applications of diode lasers to molecular fluorescence and absorption spectroscopy in the UV-visible spectral region (SHG: second-harmonic generation; SFM: sum-frequency mixing).

Species	Wavelength	Light source	Absorption	Fluorescence
NO_2	390 nm	Blue diode laser	Shock-heated NO_2-Ar mixtures [94]	
	404.3 nm	Blue diode laser	Discharge flow-tube [95]	
	640 nm	Red diode laser		Ambient air sampled to a continuous supersonic expansion [96]
	410 nm	Blue diode laser		Ambient air sampled to a low-pressure cell [97]
	406.3 nm	Blue diode laser		Ambient air sampled to an atmospheric-pressure cell [98]
NO_3	662 nm	Red diode laser		Ambient air sampled to a continuous supersonic expansion [99]
CH	426 nm	SHG of NIR diode laser	Flame [56]	Flame [56]
OH	308 nm	SFM of NIR diode laser with Ar^+ laser	Discharge-flow reactor [100]	Discharge-flow reactor [100]
	309 nm	SFM of NIR diode laser with blue diode laser	Microwave discharge [101]	
	313.5 nm	SFM of NIR diode laser with pulsed microchip laser	Flame (20 kHz rep. rate) [102]	
NO	215 nm	Frequency-quadrupled diode laser	Gas cell [103]	
	226.8 nm	SFM of blue diode laser with pulsed microchip laser	Coal-furnace exhaust [104]	
	226.6 nm		Gas cell [105]	
SO_2	215 nm	Frequency-quadrupled diode laser	Gas cell [103]	
	302 nm	SFM of blue and NIR diode lasers	Gas cell [106]	
IO	404.3 nm	Blue diode laser	Discharge flow-tube [95]	

Diode laser induced fluorescence has also been employed in the field of atmospheric chemistry to build instruments for measuring NO_2 concentration [96–98]. Nitrogen dioxide has a dense absorption spectrum covering much of the visible region. Both red [96] and blue [97,98] diode lasers have been used to excite NO_2 fluorescence. Cleary *et al.* [96] achieved a detection limit of 145 pptv NO_2 for a 1-minute averaging time by sampling of NO_2 into a supersonic expansion. The fluorescence signal was en-

hanced by collecting fluorescence from the focal position of a spherical Herriott cell. The same group also used this system for the detection of NO_3 using a 662 nm diode laser for excitation [99] in this case with a detection limit of 76 ppt min^{-1} at 8% accuracy. The instrument was used in field measurements of NO_2 and N_2O_5 concentrations east of San Francisco Bay (the latter by thermal decomposition to NO_3) [107]. An NO_2 fluorescence instrument based on a blue diode laser was built by Taketani *et al.* [97]. The excitation at 410 nm takes advantage of the higher absorption cross-section than in the red part of the visible spectrum. By sampling ambient air to a low-pressure cell, a detection limit of 390 pptv min^{-1} was achieved [97]. This is slightly less sensitive than the instrument of Cleary *et al.* [96] but avoids the use of a supersonic expansion and a Herriott cell. The laser diode was pulsed at a repetition rate of 100 kHz and a dynode gate was applied to the photomultiplier to temporally discriminate against scattered incident light [97]. This system was used for field measurements of atmospheric NO_2 concentrations at Toyokawa in Japan [108]. More recently, an instrument was developed for diode LIF detection of NO_2 at atmospheric pressure without the need for gated detection but with a less favourable sensitivity of 2000 ppt min^{-1} [98]. The use of diode laser induced fluorescence for field measurements of troposphere composition represents a mature application of the technique and has the potential to be applied to other species of importance in atmospheric chemistry.

6. Conclusions

Diode laser induced fluorescence is gaining prominence as a technique for applied measurements in a range of research fields. The increasing wavelength coverage of UV-blue GaN diode lasers has led to a growth in activity in this area in recent years. Although inherently single-mode diode lasers are not available in this spectral region, the use of an extended cavity provides narrow-linewidth radiation that is frequency tuneable over ranges exceeding 90 GHz. We have described strategies for wavelength-locking of these diode lasers to an external reference source and also for rapid wavelength tuning at rates of up to 10 kHz. The use of these compact light sources to probe strong electronic transitions of atoms and molecules allows very sensitive detection by fluorescence. The zero-baseline nature of fluorescence spectroscopy leads to obvious advantages over absorption sensing. A wide range of applications has been provided including the detection of metal atoms in flames, exhaust gases and plasmas and detection of molecular gases in flames and in the earth's atmosphere. Flame temperature measurements by two-line atomic fluorescence have reached maturity and provide important data for investigation of sooting flames, as well as being capable of resolving transient flame phenomena at repetition rates of several kHz. Diode laser induced fluorescence instruments have been used during field campaigns to measure tropospheric NO_2 and NO_3 concentrations. Despite these examples, there is significant potential for new applications of diode laser induced fluorescence which has the advantages of providing a compact, low-cost instrument capable of excellent sensitivity and selectivity. In Tables 1 and 2, recent measurements by diode laser absorption spectroscopy were included to indicate possible candidate species for future diode LIF measurements. These developments would be facilitated by continued developments in diode laser technol-

ogy and the increasing availability of powerful tuneable sources in the UV based on frequency doubling and mixing of diode laser sources. We have identified nanomaterials synthesis as a significant research area that could benefit from the application of diode LIF to measure metal atom precursor concentrations in flame and plasma reactors. Sensors based on diode laser induced fluorescence, together with other emerging techniques such as supercontinuum absorption spectroscopy [109,110], provide an exciting array of opportunities for novel research.

Acknowledgement

We are grateful for fruitful collaboration with Johan Hult, Robin Chrystie, Xavier Mercier and Pascale Desgroux. This work has been supported by the Royal Society, St John's College Cambridge, the Leverhulme Trust, the British Council, Université Lille 1 and the Engineering and Physical Sciences Research Council.

References

1. M. G. Allen, Meas. Sci. Tech. **9** (1998) 545.
2. P. Werle, Spectrochim. Acta A **54** (1998) 197.
3. P. A. Martin, Chem. Soc. Rev. **31** (2002) 201.
4. R. K. Hanson, Proc. Combust. Inst. **33** (2011) 1.
5. K. Kohse-Hoinghaus, R. S. Barlow, M. Alden, and J. Wolfrum, Proc. Combust. Inst. **30** (2005) 89.
6. P. Werle, Appl. Phys. B **102** (2011) 313.
7. J. B. Wills, M. N. R. Ashfold, A. J. Orr-Ewing, Y. A. Mankelevich, and N. V. Suetin, Diam. Relat. Mater. **12** (2003) 1346.
8. A. Farooq, D. F. Davidson, R. K. Hanson, L. K. Huynh, and A. Violi, Proc. Combust. Inst. **32** (2009) 247.
9. V. Hopfe, D. W. Sheel, C. I. M. A. Spee, R. Tell, P. Martin, A. Beil, M. Pemble, R. Weiss, U. Vogt, and W. Graehlert, Thin Solid Films **442** (2003) 60.
10. H. Teichert, T. Fernholz, and V. Ebert, Appl. Opt. **42** (2003) 2043.
11. L. A. Kranendonk, J. W. Walewski, T. Kim, and S. T. Sanders, Proc. Combust. Inst. **30** (2005) 1619.
12. T. Iseki, H. Tai, and K. Kimura, Meas. Sci. Tech. **11** (2000) 594.
13. D. Richter, M. Erdelyi, R. F. Curl, F. K. Tittel, C. Oppenheimer, H. J. Duffell, and M. Burton, Opt. Laser. Eng. **37** (2002) 171.
14. C. Roller, A. Fried, J. Walega, P. Weibring, and F. Tittel, Appl. Phys. B **82** (2006) 247.
15. T. Le Barbu, B. Parvitte, V. Zeninari, I. Vinogradov, O. Korablev, and G. Durry, Appl. Phys. B **82** (2006) 133.
16. C. Roller, K. Namjou, J. D. Jeffers, M. Camp, A. Mock, P. J. McCann, and J. Grego, Appl. Opt. **41** (2002) 6018.
17. E. R. Crosson, K. N. Ricci, B. A. Richman, F. C. Chilese, T. G. Owano, R. A. Provencal, M. W. Todd, J. Glasser, A. A. Kachanov, B. A. Paldus, T. G. Spence, and R. N. Zare, Anal. Chem. **74** (2002) 2003.
18. J. Reid and D. Labrie, Appl. Phys. B **26** (1981) 203.
19. P. Kluczynski, J. Gustafsson, A. M. Lindberg, and O. Axner, Spectrochim. Acta B **56** (2001) 1277.
20. K. Ruxton, A. Chakraborty, W. Johnstone, M. Lengden, G. Stewart, and K. Duffin, Sensor. Actuat. B-Chem. **150** (2010) 367.
21. H. R. Barry, L. Corner, G. Hancock, R. Peverall, and G. A. D. Ritchie, Chem. Phys. Lett. **333** (2001) 285.

22. G. Berden and R. Engeln (Eds.), *Cavity Ring-Down Spectroscopy: Techniques and Applications*, Wiley-Blackwell, Chichester (2009).
23. P. C. D. Hobbs, Appl. Opt. **36** (1997) 903.
24. T. Laurila, H. Cattaneo, T. Poyhonen, V. Koskinen, J. Kauppinen, and R. Hernberg, Appl. Phys. B **83** (2006) 285.
25. D. Sands, *Diode Lasers*, Institute of Physics Publishing, Bristol (2005).
26. Toptica Photonics, DL DFB, Tunable Distributed Feedback Diode Lasers, available from world wide web: http://www.toptica.com (cited 26 July 2011).
27. Nanoplus, DFB diode lasers from 760 nm to 2900 nm, available from world wide web: http://www.nanoplus.com/ (cited 26 July 2011).
28. Laser Components, VCSEL, available from world wide web: http://www.lasercomponents.com (cited 26 July 2011).
29. Vertilas, VCSEL Laser Diodes, available from world wide web: http://www.vertilas.com (cited 26 July 2011).
30. H. Li, R. K. Hanson, and J. B. Jeffries, Meas. Sci. Tech. **15** (2004) 1285.
31. S. Nakamura, Science **281** (1998) 956.
32. Nichia, Laser Diode, available from world wide web: http://www.nichia.co.jp/en (cited 28 July 2011).
33. C. E. Wieman and L. Hollberg, Rev. Sci. Instum. **62** (1991) 1.
34. K. B. MacAdam, A. Steinback, and C. Wieman, Am. J. Phys. **60** (1992) 1098.
35. L. Ricci, M. Weidemüller, T. Esslinger, A. Hemmerich, C. Zimmermann, V. Vuletic, W. König, and T. W. Hänsch, Opt. Commun. **117** (1995) 541.
36. F. Favre, D. Le Guen, J. C. Simon, and B. Landousies, Electron. Lett. **21** (1986) 795.
37. J. Mellis, S. A. Al-Chalabi, K. H. Cameron, R. Wyatt, J. C. Regnault, W. J. Devlin, and M. C. Brain, Electron. Lett. **24** (1988) 988.
38. T. Laurila, T. Joutsenoja, R. Hernberg, and M. Kuittinen, Appl. Opt. **41** (2002) 5632.
39. M. G. Boshier, D. Berkeland, E. A. Hinds, and V. Sandoghdar, Opt. Commun. **85** (1991) 355.
40. L. Hildebrandt, R. Knispel, S. Stry, J. R. Sacher, and F. Schael, Appl. Opt. **42** (2003) 1.
41. C. Petridis, I. D. Lindsay, D. J. M. Stothard, and M. Ebrahimzadeh, Rev. Sci. Instrum. **72** (2001) 3811.
42. I. S. Burns, J. Hult, and C. F. Kaminski, Appl. Phys. B **79** (2004) 491.
43. J. Hult, I. S. Burns, and C. F. Kaminski, Appl. Opt. **44** (2005) 3675.
44. J. I. Kim, C. Y. Park, J. Y. Yeom, E. B. Kim, and T. H. Yoon, Opt. Lett. **28** (2003) 245.
45. K. Hayasaka, Opt. Commun. **206** (2002) 401.
46. H. Stoehr, F. Mensing, J. Helmcke, and U. Sterr, Opt. Lett. **31** (2006) 736.
47. A. D. Ludlow, X. Huang, M. Notcutt, T. Zanon-Willette, S. M. Foreman, M. M. Boyd, S. Blatt, and J. Ye, Opt. Lett. **32** (2007) 641.
48. J. Cariou and P. Luc, *Atlas du Spectre d'Absorption de la Molécule Tellure*, Laboratoire Aimé-Cotton, CNRS II, Orsay (1980).
49. I. S. Burns, J. Hult, and C. F. Kaminski, Spectrochim. Acta A **63** (2006) 905.
50. R. S.M Chrystie, I. S. Burns, J. Hult, and C. F. Kaminski, Opt. Lett. **34** (2009) 2492.
51. L. Levin, Opt. Lett. **27** (2002) 237.
52. L. A. Kranendonk, R. J. Bartula, and S. T. Sanders, Opt. Exp. **13** (2005) 1498.
53. J. Hult, I. S. Burns, and C. F. Kaminski, Appl. Phys. B **81** (2005) 757.
54. Y. Arita, R. Stevens, and P. Ewart, Appl. Phys. B **90** (2008) 205.
55. M. L. Hamilton, G. A. D. Ritchie, Y. Arita, and P. Ewart, Appl. Phys. B **100** (2010) 665.
56. K. A. Peterson and D. B. Oh, Opt. Lett. **24** (1999) 667.
57. A. C. Eckbreth, *Laser Diagnostics for Combustion Temperature and Species*, 2nd edn., Gordon and Breach, Amsterdam (1996).
58. K. Kohse-Hoinghaus, Prog. Energy Combust. Sci. **20** (1994) 203.
59. J. W. Daily, Prog. Energy Combust. Sci. **23** (1997) 133.
60. C. F. Kaminski, Z. Phys. Chem. **219** (2005) 747.
61. C. Schulz, Z. Phys. Chem. **219** (2005) 509.

62. R. S. M. Chrystie, Development of novel laser diagnostic techniques for the quantitative study of premixed flames, PhD thesis, University of Cambridge (2009), available from world wide web: http://www.dspace.cam.ac.uk (cited 27 July 2011).
63. S. S. Brown, Chem. Rev **103** (2003) 5219.
64. P. Werle, R. Mucke, and F. Slemr, Appl. Phys. B **57** (1993) 131.
65. C. Kaminski and P. Ewart, Appl. Phys. B **61** (1995) 585.
66. S. J. Carey, H. McCann, F. P. Hindle, K. B. Ozanyan, D. E. Winterbone, and E. Clough, Chem. Eng. J. **77** (2000) 111.
67. G. Galbács, Appl. Spec. Rev. **41** (2006) 259.
68. J. Alnis, U. Gustafsson, G. Somesfalean, and S. Svanberg, Appl. Phys. Lett. **76** (2000) 1234.
69. A. E. Carruthers, T. K. Lake, A. Shah, J. W. Allen, W. Sibbett, and K. Dholakia, Opt. Commun. **255** (2005) 261.
70. T. N. Anderson, J. K. Magnuson, and R. P. Lucht, Appl. Phys. B **87** (2007) 341.
71. W. Wang, M. M. Fejer, R. H. Hammond, M. R. Beasley, C. H. Ahn, M. L. Bortz, and T. Day, Appl. Phys. Lett. **68** (1996) 729.
72. O. M. Marago, B. Fazio, P. G. Gucciardi, and E. Arimondo, Appl. Phys. B **77** (2003) 809.
73. T. Laurila, R. Oikari, and R. Hernberg, Spectrochim. Acta B **60** (2005) 783.
74. J. Hult, I. S. Burns, and C. F. Kaminski, Opt. Lett. **29** (2004) 827.
75. E. Schlosser, J. Wolfrum, L. Hildebrandt, H. Seifert, B. Oser, and V. Ebert, Appl. Phys. B **75** (2002) 237.
76. P. E. Walters, T. E. Barber, M. W. Wensing, and J. D. Winefordner, Spectrochim. Acta B **46** (1991) 1015.
77. U. Gustafsson, J. Alnis, and S. Svanberg, Am. J. Phys. **68** (2000) 660.
78. G. Galbács, Z. Galbács, O. Axner, and Z. Geretovszky, Spectrochim. Acta B **60** (2005) 299.
79. I. S. Burns, X. Mercier, M. Wartel, R. S. M. Chrystie, J. Hult, and C. F. Kaminski, Proc. Combust. Inst. **33** (2011) 799.
80. H. Wang, Proc. Combust. Inst. **33** (2011) 41.
81. I. S. Burns, N. Lamoureux, C. F. Kaminski, J. Hult, and P. Desgroux, Appl. Phys. B **93** (2008) 907.
82. N. Omenetto, P. Benetti, and G. Rossi, Spectrochim. Acta B **27** (1972) 453.
83. J. E. Dec and J. O. Keller, Proc. Combust. Inst **21** (1986) 1737.
84. C. F. Kaminski, J. Engström, and M. Aldén, Proc. Combust. Inst. **27** (1998) 85.
85. J. Engström, J. Nygren, M. Aldén, and C. F. Kaminski, Opt. Lett. **25** (2000) 1469.
86. P. R. Medwell, Q. N. Chan, P. Kalt, Z. T. Alwahabi, B. B. Dally, and G. J. Nathan, Appl. Opt. **48** (2009) 1237.
87. J. Hult, I. S. Burns, and C. F. Kaminski, Proc. Combust. Inst. **30** (2005) 1535.
88. J. E. Sansonetti and W. C. Martin, Handbook of Basic Atomic Spectroscopic Data, NIST, available from world wide web: http://www.nist.gov/pml/data/handbook/index.cfm (cited 27 July 2011).
89. A. Faccinetto, P. Desgroux, M. Ziskind, E. Therssen, and C. Focsa, Combust. Flame **158** (2011) 227.
90. G. Cleon, T. Amodeo, A. Faccinetto, and P. Desgroux, Appl. Phys. B **104** (2011) 297.
91. I. S. Burns, J. Hult, G. Hartung, and C. F. Kaminski, *Spatially-resolved flame thermometry at kHz repetition-rates using diode lasers*, in: Proceedings of the European Combustion Meeting, Chania, Crete, Combustion Institute (2007).
92. I. S. Burns, J. Hult, G. Hartung, and C. F. Kaminski, Proc. Combust. Inst. **31** (2007) 775.
93. C. Hecht, H. Kronemayer, T. Dreier, H.Wiggers, and C. Schulz, Appl. Phys. B **94** (2009) 119.
94. J. T. C. Liu, R. K. Hanson, and J. B. Jeffries, J. Quant. Spectrosc. Ra. **72** (2002) 655.
95. V. L. Kasyutich, C. S. E. Bale, C. E. Canosa-Mas, C. Pfrang, S. Vaughan, and R. P. Wayne, Appl. Phys. B **76** (2003) 691.
96. P. A. Cleary, P. J. Wooldridge, and R. C. Cohen, Appl. Opt. **41** (2002) 6950.
97. F. Taketani, M. Kawai, K. Takahashi, and Y. Matsumi, Appl. Opt. **46** (2007) 907.
98. J. Parra and L. A. George, Appl. Opt. **48** (2009) 3355.
99. E. C. Wood, P. J. Wooldridge, J. H. Freese, T. Albrecht, and R. C. Cohen, Environ. Sci. Technol. **37** (2003) 5732.

100. D. B. Oh, Opt. Lett, **20** (1995) 100.
101. L. Corner, J. S. Gibb, G. Hancock, A. Hutchinson, V. L. Kasyutich, R. Peverall, and G. A. D. Ritchie, Appl. Phys. B **74** (2002) 441.
102. T. R. Meyer, S. Roy, T. N. Anderson, J. D. Miller, V. R. Katta, R. P. Lucht, and J. P. Gord, Appl. Opt. **44** (2005) 6729.
103. J. P. Koplow, D. A. V. Kilner, and L. Goldberg, Appl. Opt. **37** (1998) 3954.
104. T. N. Anderson, R. P. Lucht, S. Priyadarsan, K. Annamalai, and J. A. Caton, Appl. Opt. **46** (2007) 3946.
105. J. Shao, L. Lathdavong, P. Thavixay, and O. Axner, J. Opt. Soc. Am. B **24** (2007) 2294.
106. G. Somesfalean, Z. G. Zhang, M. Sjöholm, and S. Svanberg, Appl. Phys. B **80** (2005) 1021.
107. E. C. Wood, T. H. Bertram, P. J. Wooldridge, and R. C. Cohen, Atmos. Chem. Phys. **5** (2005) 483.
108. T. Nakayama, T. Ide, F. Taketani, M. Kawai, K. Takahashi, and Y. Matsumi, Atmos. Environ. **42** (2008) 1995.
109. T. Laurila, I. S. Burns, J. Hult, J. H. Miller, and C. F. Kaminski, Appl. Phys. B **102** (2011) 271.
110. S.-S. Kiwanuka, T. Laurila, and C. F. Kaminski, Anal. Chem. **82** (2010) 7498.